



# Synchronization of 2-dimensional Maps Based on Neuron Model with Time-Varying Coupling

Yoko Uwate<sup>†</sup>, Yosifhimi Nishio<sup>‡</sup> and Ruedi Stoop<sup>†</sup>

<sup>†</sup>University / ETH Zurich,  
Winterthurerstrasse 190,  
CH-8057 Zurich, Switzerland,  
Email: [yu001@ini.phys.ethz.ch](mailto:yu001@ini.phys.ethz.ch)

<sup>‡</sup>Tokushima University  
2-1 Minami-Josanjima, Tokushima, Japan  
Phone: +81-88-656-7470  
Email: [nishio@ee.tokushima-u.ac.jp](mailto:nishio@ee.tokushima-u.ac.jp)

## Abstract

Biological neurons are able to exhibit spiking and bursting behavior. The interesting phenomena is ensembles of neurons by synchronization. In this study, we investigate complex patterns observed in coupled 2-dimensional maps based on neuronal model with time-varying coupling.

## 1. Introduction

Generally, complex dynamical phenomena can be observed in networks formed by many elements with nonlinearity. Coupled Map Lattice (CML) has proposed by Kaneko and Bunimovich [1]-[5], to use as general models for the complex high-dimensional dynamics, such as biological systems, networks in DNA, economic activities, neural networks, and evolutions. We can observed the spatio-temporal patterns in CML. It is very important to make clear this mechanism of the spatio-temporal patterns for understanding complex patterns observed in natural science. Usually, the chaotic maps are used for CML and many interesting spatio-temporal patterns were observed.

Recently, a discrete map for spiking-bursting neural behavior was proposed by Rulkov [6], [7]. Rulkov map (see Fig. 1) in the form of a two-dimensional map can be useful for understanding the dynamical mechanism of oscillators in the large scale networks. And Rulkov map produce spiking-bursting behavior like real neurons. In this study, we consider that Rulkov maps are used for CML. Furthermore, we assume that the coupling strength of between the neurons is not simple and the coupling strength plays important role for whole system. We consider that the coupling strength is changed with time. Time-varying coupling is realized by switching the positive and negative values, periodically. In this study, we investigate synchronization phenomena observed in two coupled Rulkov maps with time-varying coupling, and demonstrate complex patterns observed in a chain of maps.

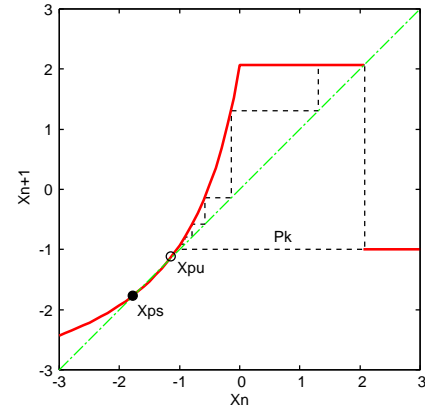


Figure 1: Rulkov map. The dashed line illustrates a superstable cycle  $P_k$ . The stable and unstable fixed points of the map are indicated by  $x_{ps}$  and  $x_{pu}$ , respectively.

## 2. Two Coupled Rulkov Maps

Consider the two coupled Rulkov maps [6] as following equation.

$$x_{i,n+1} = f(x_{i,n}, y_{i,n} + \beta_{i,n}), \quad (1)$$

$$y_{i,n+1} = y_{i,n} - \mu(x_{i,n} + 1) + \mu\sigma_i + \mu\sigma_{i,n},$$

$$f(x_n, y) = \begin{cases} \alpha/(1-x_n) + y, & x_n \leq 0 \\ \alpha + y, & 0 < x_n < \alpha + y \text{ and } x_n \leq 0 \\ -1, & x_n \geq \alpha + y \text{ or } x_{n-1} > 0, \end{cases} \quad (2)$$

where  $x$  and  $y$  are the fast and slow dynamical variables, respectively. The coupling between the cells is provided by the current flowing from one cell to the other. This coupling is modeled by

$$\beta_{i,n} = g\beta^e(x_{j,n} - x_{i,n}), \quad (3)$$

$$\sigma_{i,n} = g\sigma^e(x_{j,n} - x_{i,n}),$$

where  $g$  denotes the coupling strength. In the numerical simulations the values of the coefficients are set to be equal:  $\beta^e = 1.0$  and  $\sigma^e = 1.0$ . The other parameters has the following values:  $\mu = 0.001$ ,  $\alpha = 5.0$  and  $\sigma = 0.24$ . The coupling between the maps is symmetrical, i.e.,  $g_{ji} = g_{ij} = g$ .

### 2.1. Normal Coupling

First, we investigate basic synchronization phenomena when the normal coupling without changing the value of coupling is used. When two Rulkov maps are coupled with positive value  $g = 0.029$ , two bursting waves are synchronized at the in-phase as shown in Fig. 2. While, introduction of negative coupling  $g = -0.029$ , in this regime of synchronization shows anti-phase (see. Fig. 3). For comparison between the in-phase and the anti-phase states, the oscillation frequency of the anti-phase is faster than the in-phase state.

When three maps are coupled with negative coupling, we can observe the three-phase synchronization as shown in Fig. 4.

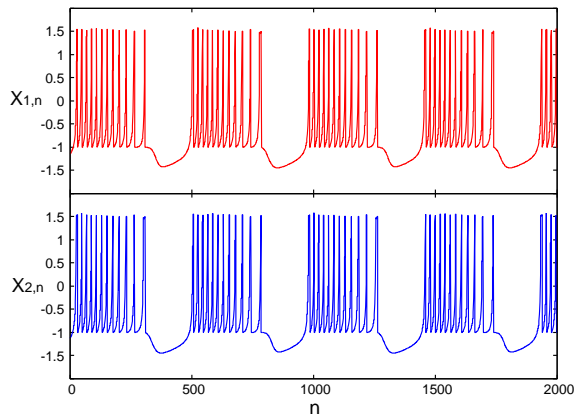


Figure 2: In-phase synchronization ( $g = 0.029$ ).

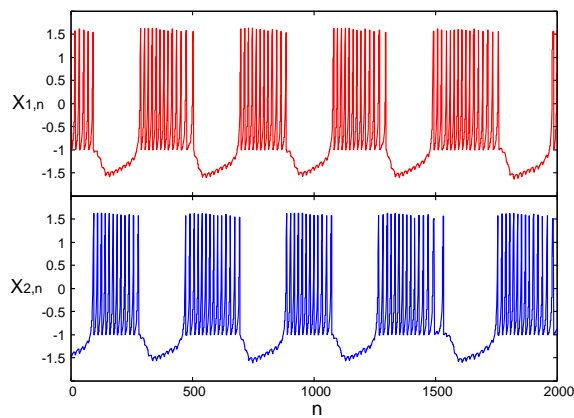


Figure 3: Anti-phase synchronization ( $g = -0.029$ ).

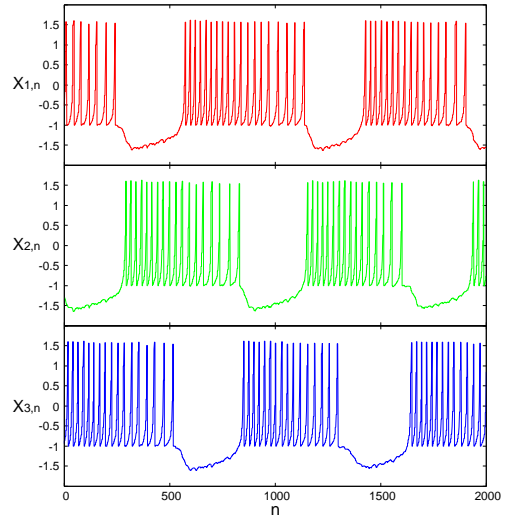


Figure 4: Three-phase synchronization ( $g = -0.029$ ).

### 2.2. Time-Varying Coupling

Figure 5 shows the characteristics of the time-varying coupling. The value of the time-varying coupling switches positive and negative periodically and  $p$  denotes the switching period.

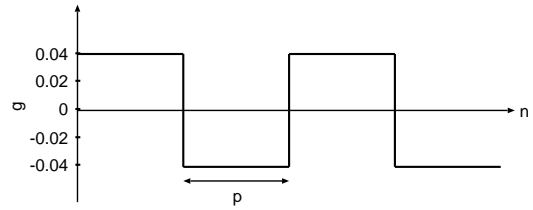


Figure 5: Characteristics of time-varying coupling.

By using the time-varying coupling, we observe the synchronization switching between in-phase and anti-phase independence on the coupling strength (when the switching period is set to  $p = 1000$ ,  $p = 200$ ) as shown in Figs. 6 and 7. Upper figure shows the two wave forms generated from two coupled Rulkov maps and lower figure shows the characteristics of the time-varying coupling. When the coupling strength has positive value, the two maps are synchronized in in-phase. While, in the case of that the coupling value is negative, two maps are synchronized in anti-phase. By switching of the value of the time-varying coupling, synchronization states also switches between the in-phase and the anti-phase states.

Next we calculated the frequency of bursting part when the iteration time is set to  $n = 1000000$  as shown in Fig. 8. From this result we can confirm that in the case of normal positive coupling, only three peaks exist. In contrast, there are many peaks by using negative coupling. When we use the time-

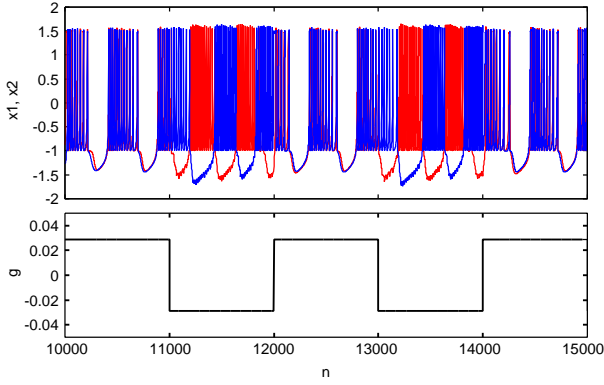


Figure 6: Switching of in-phase and anti-phase synchronization ( $p = 1000$ ).

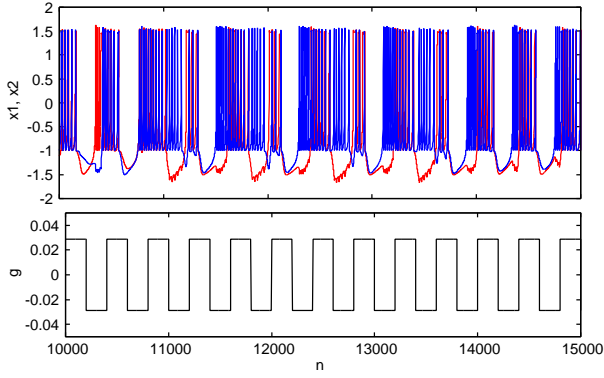


Figure 7: Switching of in-phase and anti-phase synchronization ( $p = 200$ ).

varying coupling, several peaks of bursting part are observed. Figure 9 show the simulation result of the average length of bursting part by changing period of the time-varying coupling. We confirmed two peaks of the period of time-varying coupling in this figure. We confirm that the average length of bursting part decrease, when the period of time-varying coupling becomes large.

### 3. Synchronization in a Chain of Coupled Maps

In this section, we investigate synchronization in a chain of coupled maps:

$$\begin{aligned}
 x_{i,n+1} &= f(x_{i,n}x_{i,n-1}, y_{i,n}) \\
 &\quad + \frac{1}{2}g(x_{i+1,n} - 2x_{i,n} + x_{i-1,n}), \\
 y_{i,n+1} &= y_{i,n} - \mu(x_{i,n} + 1) + \mu\sigma_i \\
 &\quad + \mu\frac{1}{2}g(x_{i+1,n} - 2x_{i,n} + x_{i-1,n}), \\
 i &= 1, \dots, N,
 \end{aligned}
 \tag{4}$$

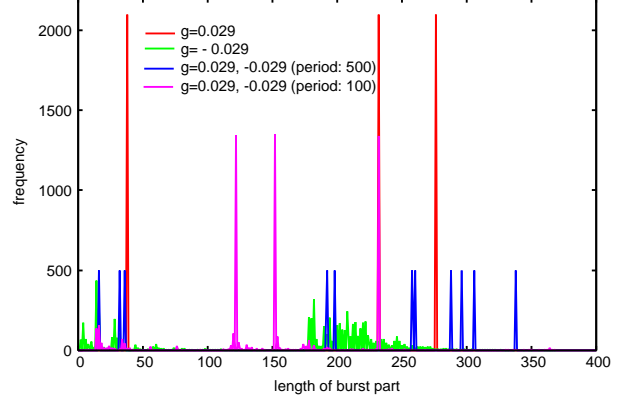


Figure 8: Histogram of length of bursting part.

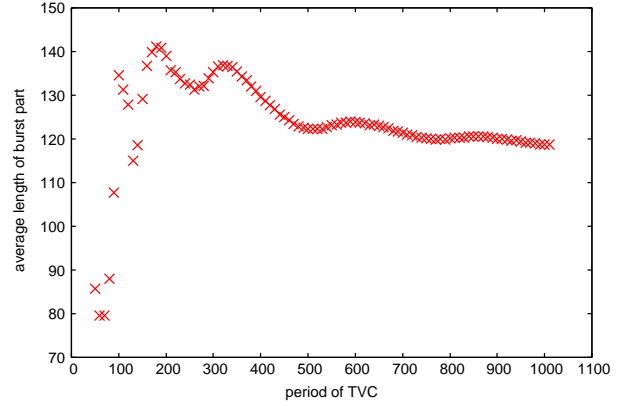


Figure 9: Average length of bursting part.

where  $x$  and  $y$  are the fast and slow dynamical variables, respectively.  $\mu = 10^{-3}$  and  $\sigma_i$  are the parameters of the individual map and  $g$  is the coupling. The function  $f()$  has the following form:

$$f(x_n, y_n) = \begin{cases} \alpha/(1 - x_n) + y_n, & x_n \leq 0, \\ \alpha + y_n, & 0 < x_n < \alpha + y_n \\ & \text{and } x_{n-1} \leq 0, \\ -1, & x_n \geq \alpha + y_n \text{ or } x_{n-1} > 0, \end{cases}
 \tag{5}$$

This model is a modification of the model presented in Sec. 2. In this simulations, we take  $\alpha = 3.5$  and  $\sigma_i$  is set for randomly distributed in the interval  $[0.15:0.16]$ . The simulation results of the space-time plot by changing period of time-varying coupling are shown in Figs. 10-12. The horizontal axis is iteration time  $n$  and the vertical axis is space  $i$ . When the time varying coupling is set to positive, the wave propagation can be observed. While, in the case of negative coupling, we confirm the random patterns are produced. By decreasing the period of time-varying coupling, the length of each region of wave propagation and random pattern becomes

shorter. Figure 13 shows the simulation result of the space-time plot when the coupling is set to  $g = \pm 0.4$  and the period of time-varying coupling is  $p = 100$ .

We consider that the interesting complex patterns can be observed by switching coupling strength.

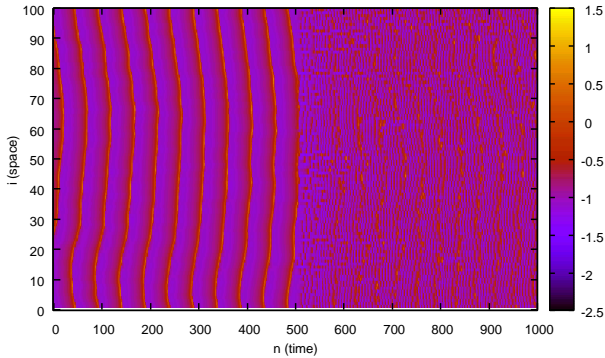


Figure 10: Space-time plots of  $x_i$ . ( $g = \pm 0.2, p = 500$ ).

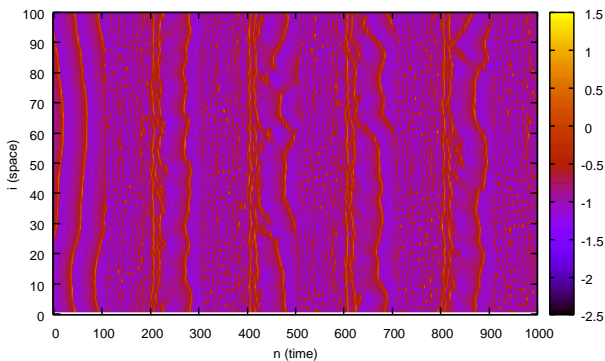


Figure 11: Space-time plots of  $x_i$ . ( $g = \pm 0.2, p = 100$ ).

#### 4. Conclusions

In this study, we have investigated synchronization phenomena observed in two coupled Rulkov maps with time-varying coupling, and demonstrated complex patterns observed in a chain of maps. In the future works, we investigate synchronization of maps by the other coupling methods such as the chemical and diffusion coupling.

#### References

[1] K. Kaneko, "Spatiotemporal Intermittency in Coupled Map Lattice," *Prog. Theor. Phys.*, vol.75, no.5, pp.1033–1044, 1985.

[2] L. A. Bunimovich and Ya. G. Sinai, "Spacetime Chaos in Coupled Map Lattices," *Nonlinearity* 1, no.4, pp.491–516, 1988.

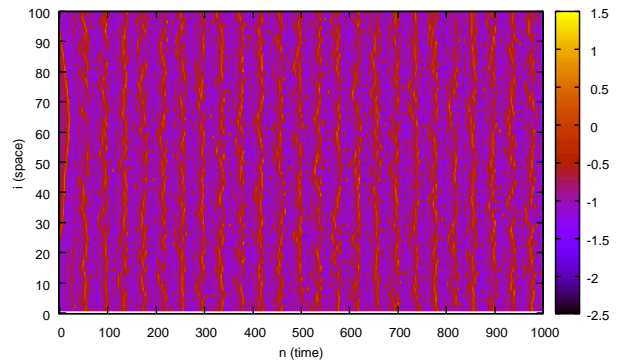


Figure 12: Space-time plots of  $x_i$ . ( $g = \pm 0.2, p = 20$ ).

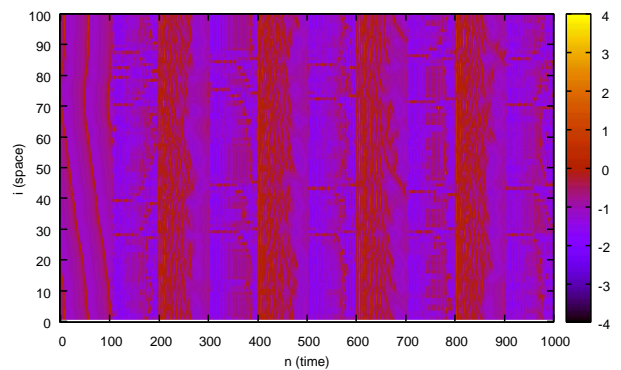


Figure 13: Space-time plots of  $x_i$ . ( $g = \pm 0.4, p = 100$ ).

[3] K. Kaneko, "Pattern Dynamics in Spatiotemporal Chaos," *Physica D*, vol.34, pp.1–41, 1989.

[4] K. Kaneko, "Spatiotemporal Chaos in One- and Two-Dimensional Coupled Map Lattice," *Physica D*, vol.37, pp.60–82, 1989.

[5] K. Kaneko, "Simulating Physics with Coupled Map Lattice - Pattern Dynamics, Information Flow, and Thermodynamics of Spatiotemporal Chaos," *Formation, Dynamics, and Statistics of Patterns*, World Sci., pp.1–52, 1990.

[6] N. F. Rulkov, "Modeling of Spiking-Bursting Neural Behavior using Two-dimensional Map," *Physical Rev., E*, vol. 65, 041922, 2002.

[7] N. F. Rulkov, I. Timofeev and M. Bazhenov, "Oscillations in Large-Scale Cortical Networks: Map-Based Model," *Journal of Computational Neuroscience* vol. 17 pp. 203–223, 2004.